Annals of Botany **114**: 35–45, 2014
doi:10.1093/aob/mcu073, available online at www.aob.oxfordjournals.org

ANNALS OF BOTANY
Founded 1887

Programmed cell death in kiwifruit stigmatic arms and its relationship to the effective pollination period and the progamic phase

Yolanda Ferradás[1], Marián López[1], Manuel Rey[2] and M[a] Victoria González[1,*]

[1]*Departamento de Fisiología Vegetal, Facultad de Farmacia, Universidad de Santiago, Campus Sur, 15872 Santiago de Compostela, Spain and* [2]*Departamento de Biología Vegetal y Ciencia del Suelo, Facultad de Biología, Universidad de Vigo, 36310 Vigo, Spain*

** For correspondence. E-mail mvictoria.gonzalez@usc.es*

Received: 14 November 2013 Returned for revision: 12 February 2014 Accepted: 18 March 2014 Published electronically: 29 April 2014

• **Background and Aims** Kiwifruit is a crop with a highly successful reproductive performance, which is impaired by the short effective pollination period of female flowers. This study investigates whether the degenerative processes observed in both pollinated and non-pollinated flowers after anthesis may be considered to be programmed cell death (PCD).

• **Methods** Features of PCD in kiwifruit, *Actinidia chinensis* var. *deliciosa*, were studied in both non-pollinated and pollinated stigmatic arms using transmission electron microscopy, DAPI (4′,6-diamidino-2-phenylindole) staining, TUNEL (terminal deoxynucleotidyl transferase-mediated dUTP nick end labelling) assays, DNA gel electrophoresis and caspase-like activity assays.

• **Key Results** In the secretory tissues of the stigmatic arms, cell organelles disintegrated sequentially while progressive vacuolization was detected. At the same time, chromatin condensation, nuclear deformation, and DNA fragmentation and degradation were observed. These features were detected in both non-pollinated and pollinated stigmatic arms; they were evident in the stigmas of pollinated flowers by the second day after anthesis but only by 4 d after anthesis in non-pollinated flowers. In addition, in pollinated stigmatic arms, these features were first initiated in the stigma and gradually progressed through the style, consistent with pollen tube growth. This timing of events was also observed in both non-pollinated and pollinated stigmatic arms for caspase-3-like activity.

• **Conclusions** The data provide evidence to support the hypothesis that PCD processes occurring in the secretory tissue of non-pollinated kiwifruit stigmatic arms could be the origin for the observed short effective pollination period. The results obtained in the secretory tissue of pollinated kiwifruit stigmatic arms upon pollination support the idea that PCD might be accelerated by pollination, pointing to the involvement of PCD during the progamic phase.

Key words: programmed cell death, PCD, *Actinidia chinensis* var. *deliciosa*, effective pollination period, EPP, pollen–pistil interaction, reproductive biology, TUNEL assay, DAPI staining, TEM, caspase-like activity.

INTRODUCTION

Eukaryotes such as plants, animals and yeast have all evolved ways of undergoing cellular suicide that are known as programmed cell death (PCD; Lam, 2004). PCD is the active process of cell death that occurs during development and in response to environmental cues (Greenberg, 1996), although it must not be confused with necrosis, which refers to accidental cell death in response to an injurious environmental factor (Coimbra *et al*., 2004). PCD allows the selective elimination of unwanted cells (Ellis *et al*., 1991) and plays an important role in cell and tissue homeostasis and specialization, tissue sculpting and disease (Pennell and Lamb, 1997).

Programmed cell death is an integral part of plant development and defence. It occurs at all stages of the life cycle, from fertilization of the ovule to death of the whole plant (van Doorn and Woltering, 2005). In fact, the term PCD is widely used to describe most cases of death observed in plants, leading to much confusion. Numerous studies have been conducted to better define plant PCD. Several hallmarks are currently considered indicative of PCD in plants, such as chromatin condensation, DNA fragmentation into large fragments and DNA laddering, altered nuclear morphology, ultrastructural changes [vacuolar increase, swelling of mitochondria and the endoplasmic reticulum (ER), and protoplast shrinkage] and caspase-like activity. These hallmarks have been used both to categorize plant PCD in relation to the types described in animals (van Doorn and Woltering, 2005; Collazo *et al*., 2006; Della Mea *et al*., 2007) and more recently to discuss cell death categories in plants (Love *et al*., 2008; Reape *et al*., 2008; Hara-Nishimura and Hatsugai, 2011; van Doorn *et al*., 2011).

The mechanisms of PCD in plant development have been intensively studied and characterized in detail in several systems, including reproductive development processes such as self-incompatibility (Thomas and Franklin-Tong, 2004; Bosch and Franklin-Tong, 2008; Bosch *et al*., 2010), death of floral organs (Coimbra *et al*., 2004; Rogers, 2006), pollen sterility (Coimbra *et al*., 2004; Falasca *et al*., 2013) and pollen–pistil interaction during compatible pollination (Wu and Cheung, 2000; Hiratsuka *et al*., 2002; Serrano *et al*., 2010).

Pollination is a yield-limiting process in kiwifruit since fruit weight is closely related to the number of seeds. *Actinidia chinensis* var. *deliciosa* is a functionally dioecious species with female flowers producing unviable pollen (Coimbra *et al*.,

2004; Falasca *et al*., 2013). Kiwifruit female flowers need to support the growth of >1000 pollen tubes that reach the base of the style only 48 h after pollination, and the first fertilized ovules are observed 24 h later (González *et al*., 1995*a*). Pollen tube growth is supported by an abundant secretion present from anthesis in the intercellular spaces of female secretory tissues throughout the entire pathway, providing pollen tube nutrition and guidance (González *et al*., 1996). These processes generate a progressive deterioration of the female tissues which finally produce the end of the effective pollination period (EPP) defined as the capability to set fruit after pollinating flowers (González *et al*., 1995*a*, *b*).

This progressive deterioration of the female tissues appears to be developmentally regulated because it has been detected in both non-pollinated and pollinated flowers, although it is accelerated by pollination (González *et al*., 1996). It can play an important role in signalling and recognition, pathogen defence, pollen capture and adhesion, and pollen tube growth (Hiscock and Allen, 2008). This deterioration was interpreted as PCD in stigmatic and stylar tissues, with pollination considered an inducer during pollen–pistil interaction (Wu and Cheung, 2000).

The aim of our report is to provide new insights into the nature of the processes occurring in the female tissues and the influence of pollination on these processes. To investigate this, we studied the pattern of deterioration in the stigmatic arms of pollinated and non-pollinated female flowers of kiwifruit. The characterization of PCD in these tissues was performed by studying established hallmarks in plant cells for PCD, such as ultramicroscopic cellular alterations, chromatin condensation, and nuclear DNA cleavage and fragmentation, and by determination of caspase-like activity.

MATERIALS AND METHODS

Plant material

This work was carried out on mature female vines of kiwifruit, *Actinidia chinensis* var. *deliciosa* (A.Chev.) A.Chev, 'Hayward' growing in a commercial orchard located in north-western Spain (Galicia) and operated by Kiwi Atlántico S.A.

Pollinations were performed with pollen from mature male vines grown in the same orchard. Pollen was obtained from male flowers collected 1 d prior to anthesis and stored at −20 °C until use. Female flowers were bagged before anthesis (the day petals open and stigmatic arms are exposed for pollination) to prevent uncontrolled pollination, and they were pollinated on the day of anthesis. A batch of flowers was similarly treated but left unpollinated to follow the development of the stigmatic arms within them. Self-pollination is not possible in this species because female cultivars produce unviable pollen (Coimbra *et al*., 2004; Falasca *et al*., 2013).

Flowers inside the bags were collected for analysis from 2 d before anthesis until 5 d following anthesis at daily intervals during the flowering period of three consecutive years. Thirty flowers per day and per treatment were collected in liquid N_2 and stored at −80 °C until use in molecular experiments. Additionally ten flowers per day and per treatment were collected for histological studies. From these, five flowers were fixed in 3:1 ethanol:acetic acid, transferred to 75 % ethanol (Williams *et al*., 1999) and stored at 4 °C until use. The other five were fixed in 2·5 % glutaraldehyde in 30 mM phosphate buffer (Sabatini *et al*., 1963) at pH 6·8 and stored at 4 °C in fixative until use.

Toluidine blue staining

Fixed stigmatic arms were embedded in paraffin after dehydration through a tertiary butyl alcohol series. They were serially sectioned into 10 μm thick slices. To observe variations in the general structure of the tissues, the paraffin sections were stained with 0·1 % Toluidine Blue Acid (Panreac, Barcelona, Spain) in 0·1 M acetate buffer, pH 4·4, and then mounted in Eukit (Fluka, Buchs, Switzerland). Sections were visualized with a Leica TCS-SP2 optical microscope (Wetzlar, Germany).

Transmission electron microscopy (TEM)

For TEM, fixed stigmatic arms were washed in 0·025 M cacodylate buffer (pH 7·4) and then post-fixed in 1 % OsO_4 in 0·1 M cacodylate buffer (pH 7·4) for 1 h. After fixation, samples were dehydrated in graded ethanol solutions, including one bath of 70 % ethanol, and then embedded in Epon resin (TED-PELLA Inc., Redding, CA, USA). Ultrathin sections were cut on a Leica UltraCut R ultramicrotome. Sections were examined using a Philips CM12 transmission electron microcope (Mahwah, NJ, USA).

DAPI assay

To assay changes in the condensed chromatin, fixed stigmatic arms were dehydrated through an ethanol series, embedded in Historesin (Reichert-Jung, Heidelberg, Germany) according to the manufacturer's instructions and finally sectioned into 2·5 μm thick slices. Historesin sections were stained with a 1 μg mL^{-1} DAPI (4′,6-diamidino-2-phenylindole; SERVA, Heidelberg, Germany) solution in phosphate-buffered saline (PBS) and Triton X-100 (1 %) (Sigma, St. Louis, MO, USA) for 10 min at room temperature in darkness, then rinsed in running water and mounted in 50 % glycerol in PBS. Sections were examined in a Leica TCS-SP2 confocal microscope using an excitation wavelength of 405 nm and detection in the range of 415–490 nm.

Nuclei were counted in four microscope fields in at least three DAPI-stained stigmatic arms per day and per treatment. The results are shown as the percentage (mean ± s.e.) of the observed nuclei with respect to those observed at anthesis (100 %). Data were statistically analysed using one-way analysis of variance (ANOVA) with a Mann–Whitney *U*-test ($P < 0·05$).

TUNEL assay

For *in situ* detection of DNA fragmentation, paraffin sections of 10 μm thickness were mounted on microscope slides coated with TESPA (Sigma). Terminal deoxynucleotidyl transferase-mediated dUTP nick end labelling (TUNEL) assays were performed using an ApoAlert® DNA Fragmentation Assay Kit (Clontech, Mountain View, CA, USA) according to the manufacturer's instructions with the following modification to increase tissue permeability. Sections were deparaffinized and subsequently pre-treated with 2 % cellulase Onozuka RS (Duchefa Biochemie, Haarlem, The Netherlands) in PBS for 90 min at 37 °C, washed in PBS and incubated in 0·5 % Triton X-100

(Sigma) in PBS for 20 min at room temperature. Incubation with 20 μg mL^{-1} proteinase K (Sigma) was optimized for 30 min at 37 °C. Positive controls were treated with 1500 U mL^{-1} DNase I (TAKARA BIO INC., Otsu, Shiga, Japan) for 20 min at 37 °C following the suggestions presented in the *In Situ* Cell Death Detection Kit, Fluorescein (Roche Applied Science, Mannheim, Germany).

All sections were counterstained with 0·5 μg mL^{-1} propidium iodide (PI; Sigma) in PBS for 5 min to visualize all nuclei. Finally, Anti-Fade reagent (Citifluor Solid Mountant kit, AgarScientific, Stansted, UK) was used to mount the slides to protect the fluorescent signal. Sections were examined in a Leica TCS-SP2 confocal microscope. Fluorescence was detected using an excitation wavelength of 488 nm for the TUNEL reaction and 561 nm for PI and detection in the range of 492–550 nm for the TUNEL reaction and 581–625 nm for PI.

The number of TUNEL-positive nuclei was estimated over a total of 100 nuclei stained with TUNEL and counterstained with PI; the nuclei were counted in six microscopic fields of at least two stigmatic arms per day and per treatment. The results are shown as the percentage of TUNEL-positive nuclei (mean ± s.e.) over the total. Data were statistically analysed using one-way ANOVA with a Mann–Whitney *U*-test ($P < 0{\cdot}05$).

DNA isolation and electrophoresis

Total DNA was isolated from 100 mg of stigmatic arms. DNA extractions were carried out using the DNeasy Plant Mini Kit (Qiagen, Hilden, Germany) according to the manufacturer's instructions. Genomic DNA (1 μg per lane) was separated using agarose gels (0·8, 2 and 3 %, Bio-Rad, Hercules, CA, USA), TreviGel™ 500 (1·5 %, Trevigen, Gaithersburg, MD, USA) or PCR CheckIt™ Gel (Elchrom Scientific, Cham, Switzerland). Double-stranded DNA fragments were stained with 5 % ethidium bromide or SYBR® Green I (Sigma), and visualized and photographed with a Gel Doc XR system (Bio-Rad) using the application Quantity One version 4.6.1 (Bio-Rad).

Protein isolation and caspase-3-like activity assay

Total protein extracts were obtained from 100 mg of stigmatic arms from pollinated and non-pollinated flowers collected daily before and after anthesis, closed floral buds, and mature and recently expanded leaves, following the protocol described by Lombardi *et al*. (2007). Proteolytic activity was measured in 500 μL reaction mixtures containing 250 μg of protein and 200 μM caspase-3 substrate [Ac-DEVD-pNA dissolved in dimethylsulfoxide (DMSO)] in 50 mM acetate buffer, pH 4·5. Reactions were incubated for 3 h at 30 °C, and absorbance at 405 nm was then measured against a blank containing only buffer and substrate. A control of each sample was made without substrate. All assays were performed using three protein extractions per day and per treatment, with spectrophotometric measurements made in duplicate. The experiments were repeated three times. In the relevant experiments, inhibitors were added to the respective reaction mixtures and incubated for 20 min at 30 °C prior to the addition of the substrates. The results are shown as the means ± s.e. of the percentage activity with respect to the maximum, which was a control sample without inhibitor. Data were statistically analysed using one-way ANOVA with a Mann-Whitney *U*-test ($P < 0{\cdot}05$).

The inhibitors used were 300 μM Ac-DEVD-CHO (caspase-3 inhibitor), 500 μM *trans*-epoxysuccinyl-L-leucylamido(4-guanidino) butane (E-64), 500 μM pepstatin A and 500 μM phenylmethylsulfonyl fluoride (PMSF). Both substrates and inhibitors were purchased from Enzo Life Sciences (Lausen, Switzerland). As some protease substrates and inhibitors were dissolved in organic solvents (DMSO or ethanol), the effect of these solvents on the caspase-like protease activity was also tested.

RESULTS

Morphology and microscopic structure of pollinated and non-pollinated stigmatic arms

Stereomicroscopic images of excised stigmatic arms showed changes in their morphology with time after anthesis, with remarkable differences between pollinated and non-pollinated flowers (Fig. 1). Stigmatic arms were turgid and white during the first 3 d after anthesis and then they turned gradually brown in colour from the stigma towards the base of the style (Fig. 1D–I). Five days after anthesis, almost all the upper half of non-pollinated stigmatic arms was brown (Fig. 1F), whereas pollinated stigmatic arms were brown throughout their whole length (Fig. 1I).

Macroscopic observations were supported by microscopic analysis of the tissues in semi-thin sections of stigmas and styles stained with toluidine blue. A semi-thin section of stigma is presented in Fig. 1A showing the papillar surface, cortical and vascular tissues and the secretory tissue. This secretory tissue at the stigma is continuous with the transmitting tissue at the level of the style (Fig. 1B). Secretory tissue at the stigma and transmitting tissue at the style showed a conspicuous secretion in the extracellular matrix in non-pollinated stigmatic arms (Fig. 1A, B). In contrast, secretion was absent in pollinated stigmatic arms, consistent with pollen tube passage through the stigma during the first day after anthesis (Fig. 1J) and at the base of the style during the second day after anthesis (Fig. 1 K). Complete tissue deterioration was observed by the fifth day after pollination at both the stigma (Fig. 1L) and style (data not shown), while in the stigmatic arms of non-pollinated flowers, tissues scarcely showed signs of deterioration (Fig. 1C).

The ultrastructural details (Fig. 2A–D) of the different tissues in the stigma and style at anthesis previously described were further studied using TEM. Figure 2A shows unicellular papillae surrounded by a continuous and festooned cuticle, whereas Fig. 2B shows a cell completely filled with a large vacuole from the cortical tissue. In the secretory tissue, the outer cells contained nuclei with conspicuous nucleoli and scattered chromatin, and a cytoplasm with well-conserved organelles (Fig. 2C). However, the inner cells showed a dense cytoplasm rich in starch reserves, and there was a conspicuous extracellular secretion (Fig. 2D). During the days following anthesis, these inner cells showed the modifications described below, with differences between non-pollinated and pollinated flowers.

In the secretory tissue of stigmas from non-pollinated flowers, the secretion was still present in the extracellular matrix 2 d after anthesis, while starch reserves disappeared as the cells became much more vacuolated (Fig. 2E). Cells contained nuclei with slightly condensed chromatin, while organelles such as the Golgi apparatus, ER with attached ribosomes and oval-shaped

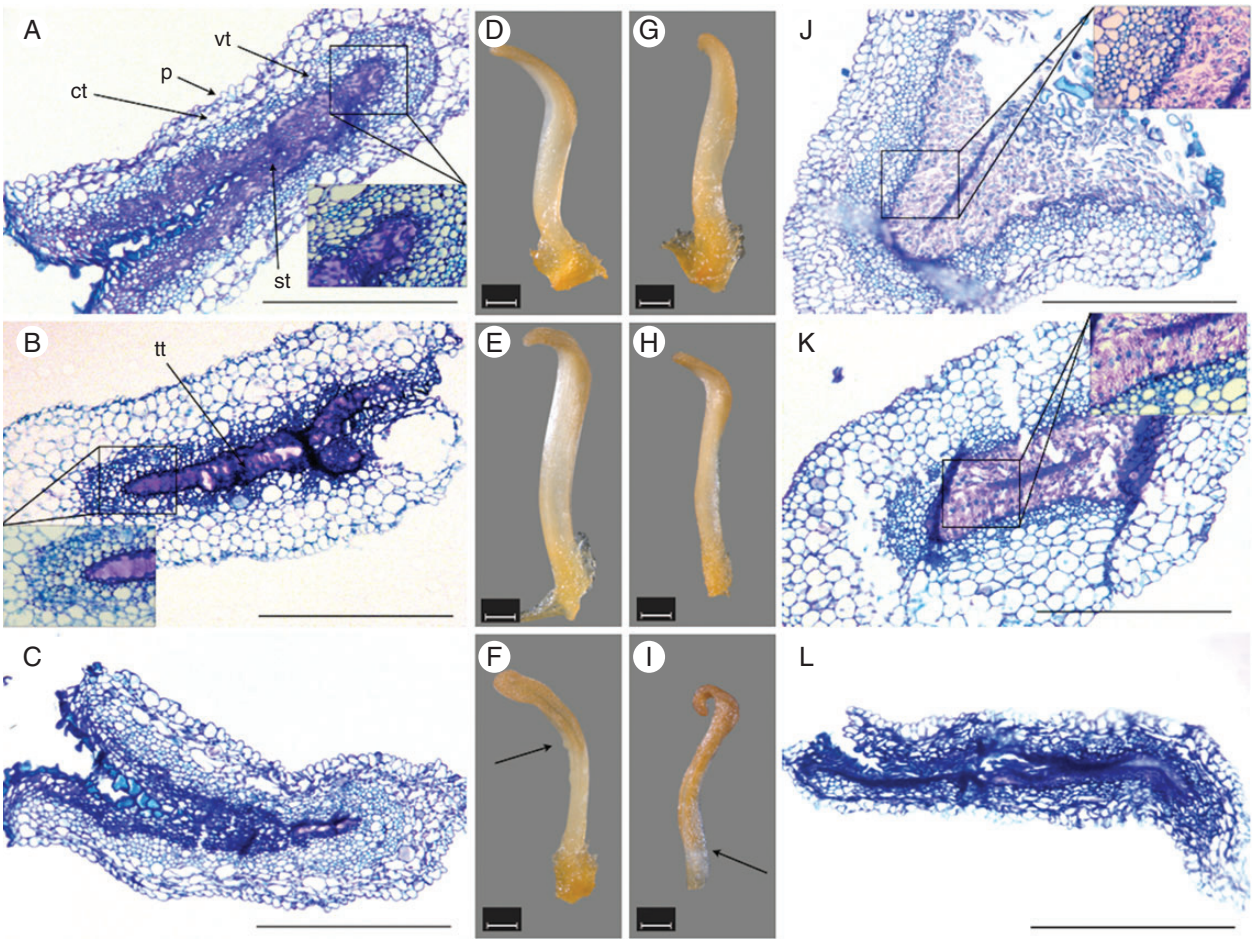

FIG. 1. Microphotographs of stigma and style sections from the stigmatic arms of kiwifruit flowers stained with toluidine blue and their corresponding stereomicroscope images. (A–C) Non-pollinated stigmatic arms sectioned at the level of the stigma 1 d after anthesis, showing that the secretion remains unaltered (inset) in (A); at the level of the style 2 d after anthesis, showing that the secretion remains unaltered (inset) in (B); and at the level of the stigma 5 d after anthesis in (C). (D–F) Stigmatic arms from non-pollinated flowers collected at days 1, 2 and 5 after anthesis showing a progressive pale-coloured browning (arrow). (G–I) Stigmatic arms from pollinated flowers collected at days 1, 2 and 5 after pollination, showing a progressive browning (arrow). (J–L) Pollinated stigmatic arms sectioned at the level of the stigma 1 d after pollination showing the disappearance of secretion after pollen tube passage (inset) in (J), at the level of the style 2 d after pollination showing the disappearance of secretion after pollen tube passage (inset) in (K), at the level of the stigma 5 d after pollination and appearing completely degenerated in (L). Scale bars (A–C, J–L) = 500 μm; (D–I) = 1 mm. Abbreviations: ct, cortical tissue; p, papillae; st, secretory tissue; tt, transmitting tissue; vt, vascular tissue.

mitochondria were still observed (Fig. 2F). However, 4 d after anthesis, some cells exhibited collapse of the vacuolar membrane, swollen, less electron-dense mitochondria with a more spherical shape and a swollen ER with few ribosomes adhered to its membrane (Fig. 2G), whereas other cells were degenerated and had a shrunken protoplast with cell membranes detached from the cell wall and small vesicles in the space between them (Fig. 2H).

In the stigmas of pollinated flowers at 1 d after anthesis, cells of the secretory tissue showed structural changes consistent with pollen tube passage. In these cells (Fig. 2I), nuclei exhibited condensed chromatin but still showed a double membrane structure, organelles such as mitochondria appeared less electron dense and less oval in shape, and starch reserves were reduced or disappeared and were replaced by vacuoles. Other changes observed were that plasma membrane started to shrink and detach from the cell wall and the extracellular secretion disappeared (Fig. 2I). Two days after anthesis, in the stigma of pollinated flowers, the secretory tissue collapsed, with cells having large vacuoles and the plasma membrane separated from the cell wall because of protoplast shrinkage (Fig. 2J). Some cells showed nuclei still with condensed chromatin and a double membrane structure, but mitochondria were spherical in shape and accumulated close to the plasma membrane along with other organelles such as the ER and Golgi apparatus (Fig. 2K). Other cells showed degenerated organelles and the rupture of the tonoplast (Fig. 2L).

Nuclear changes in the condensed chromatin

Staining with DAPI was used to detect chromatin condensation in nuclei from cells of the stigmatic secretory tissue (Fig. 3) and cells of the transmitting tissue at the base of the style from pollinated and non-pollinated flowers at different stages after anthesis. In the stigma of flowers at anthesis, nuclei appeared spherical with dispersed chromatin (data not shown), while this nuclear pattern changed gradually after anthesis, in both non-pollinated and pollinated flowers. In the cells of the secretory tissue from non-pollinated stigmas, chromatin tended

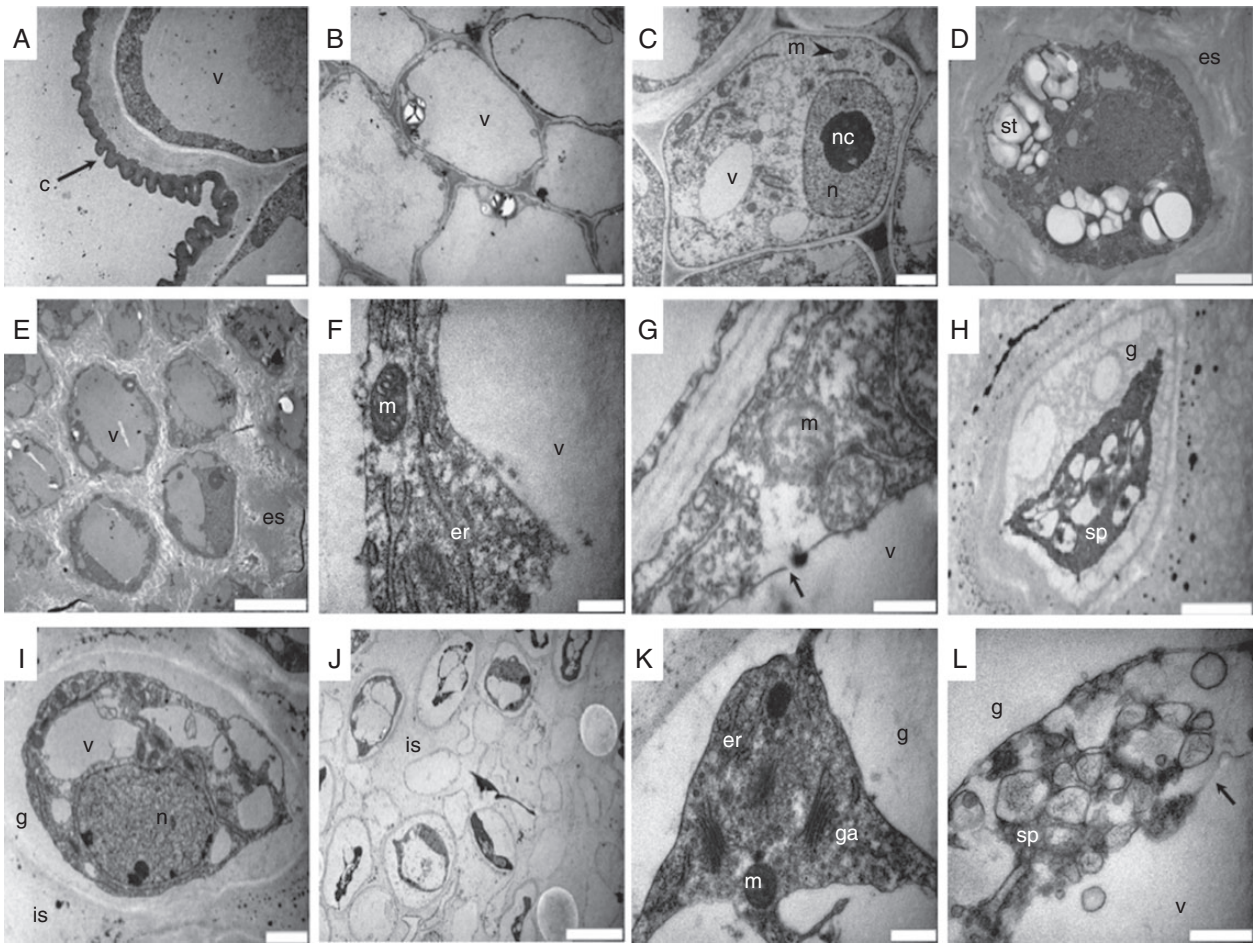

FIG. 2. Transmission electron micrographs of stigmas from non-pollinated and pollinated kiwifruit stigmatic arms. (A–D) Stigmas at anthesis. (A) Unicellular papillae surrounded by a continuous and festooned cuticle; (B) cortical cells completely filled with a large vacuole; (C) outer cells of the secretory tissue showing very active nuclei with conspicuous nucleoli and scattered chromatin; (D) inner cells of the secretory tissue presenting a dense cytoplasm rich in starch reserves, and with an conspicuous extracellular secretion. (E, F) Inner secretory cells of non-pollinated stigmas 2 d after anthesis showing greater vacuolization with less starch reserves, a nucleus with more condensed chromatin in (E), and organelles with a well-conserved structure in (F). (G, H) Inner secretory cells of non-pollinated stigmas 4 d after anthesis showing changes in the organelles in (G) or becoming more degenerated with a shrunken protoplasm and a gap between the cell membrane and cell wall in (H). (I) Inner secretory tissue of pollinated stigmas showing cells with condensed chromatin 1 d after anthesis, large vacuoles replacing starch reserves and shrunken plasma membranes detached from the cell wall. (J–L) Inner secretory tissue of pollinated stigmas showing, 2 d after anthesis, cells filled by large vacuoles with protoplast shrinkage in (J), with organelles (spherical mitochondria, endoplasmic reticulum and Golgi apparatus) accumulated in the cell periphery in (K) or with organelles completely degenerated in (L). Scale bars: (A, C, H, I) = 2 μm; (B, E, J) = 10 μm; (D) = 5 μm; (F, G, K, L) = 0·5 μm. Abbreviations: c, cuticle; er, endoplasmic reticulum; es, extracellular secretion; g, gap; ga, Golgi apparatus; is, intercellular space; m, mitochondria; n, nucleus; nc, nucleolus; sp, shrunken protoplast; st, starch; v, vacuole. Arrows indicate tonoplast rupture in (G) and (L).

to become slightly condensed (Fig. 3A) during the first 3 d, and then it appeared more clearly condensed from the fourth day after anthesis (Fig. 3B, C). However, in pollinated flowers, nuclei showed condensed chromatin on the second day (Fig. 3D), becoming tubular in shape by the fourth day (Fig. 3E), and completely disrupted by day 5 (Fig. 3F). The changes in chromatin condensation and nuclear shape described for the secretory tissue at the stigma were also observed in the cells of the transmitting tissue at the base of the style (data not shown).

A remarkable reduction in the number of nuclei in the cells of the secretory tissue of stigmas from both pollinated and non-pollinated flowers with respect to anthesis was also observed (Fig. 3G). In non-pollinated flowers collected 4 d after anthesis, a significant reduction in the number of nuclei (50 %) was detected, only 35 % of the nuclei being observed by the fifth day. This significant reduction has also been observed in pollinated flowers, where 55 % of the nuclei were present on the second day after anthesis and only 25 and 20 % on the fourth and fifth days, respectively. The reduction in the number of nuclei was also observed in the transmitting tissue at the base of the style, following exactly the same timing as described for the stigmas, except for pollinated flowers on the first day after anthesis (Fig. 3G). By this time, this reduction was lower in the styles, with 90 % of nuclei observed, than in the stigmas (80 %).

DNA cleavage assay

A TUNEL assay was used to evaluate *in situ* DNA cleavage in paraffin sections of the stigmatic arms from pollinated and non-pollinated flowers at different stages after anthesis (Fig. 4).

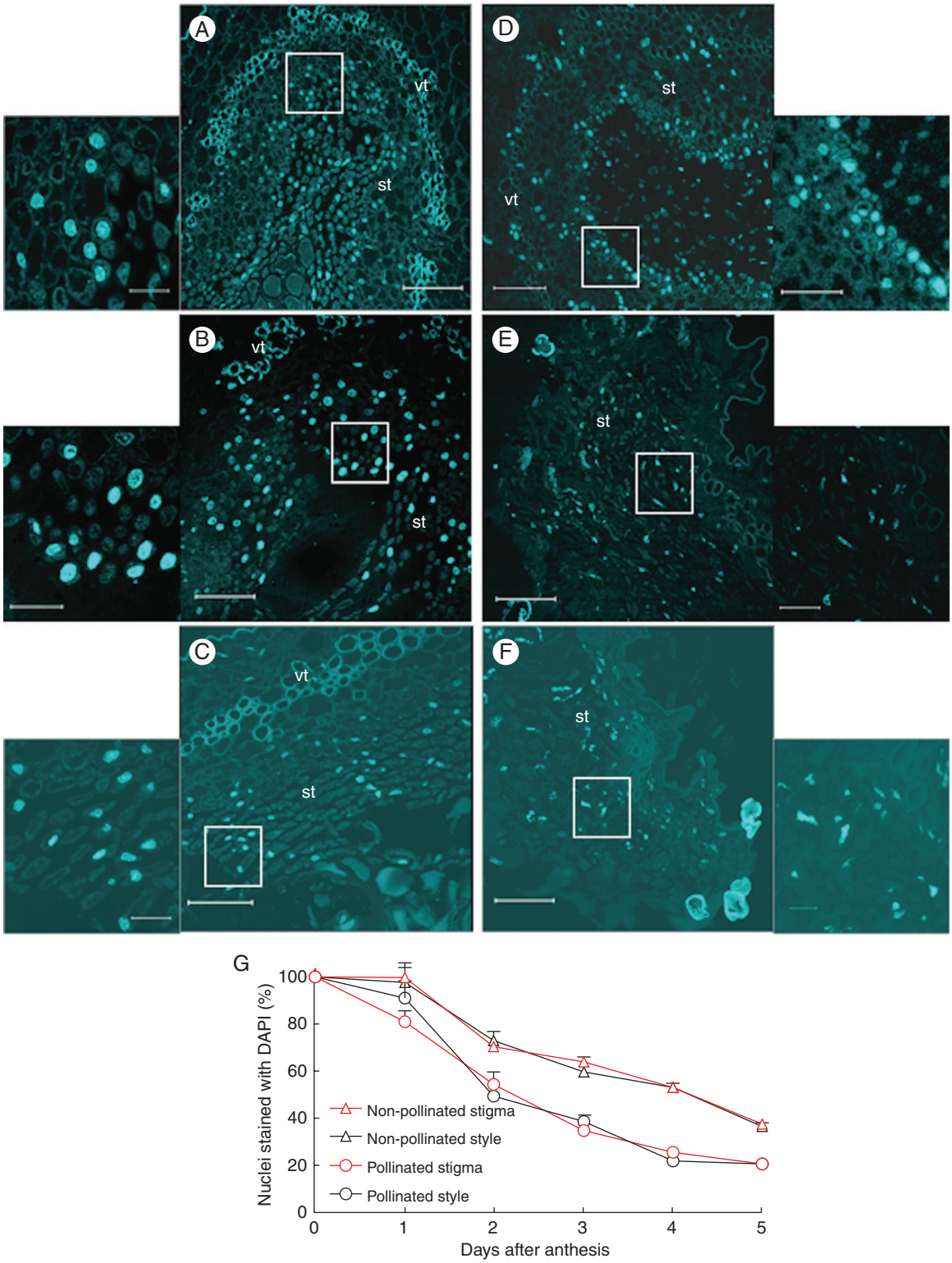

FIG. 3. Detection of chromatin condensation using DAPI staining in sections from the stigmatic arms of kiwifruit flowers collected at 2, 4 and 5 d after anthesis (A–F). (A–C) Non-pollinated and (D–F) pollinated stigmatic arms sectioned at the level of the stigma, showing progressive condensation of the chromatin and a change in the shape of the nuclei. Magnified sections are given to the side of each image, and show the area indicated by the box. (G) Percentage of nuclei stained with DAPI in sections at the levels of the stigma and the base of the style from non-pollinated and pollinated flowers. Data represent the percentage (mean ± s.e.) in respect to anthesis (100 %) of the nuclei counted in four microscope fields in at least three stigmatic arms per day and per treatment. Scale bars (A–F) = 75 μm; insets = 15 μm. Abbreviations: st, secretory tissue; vt, vascular tissue.

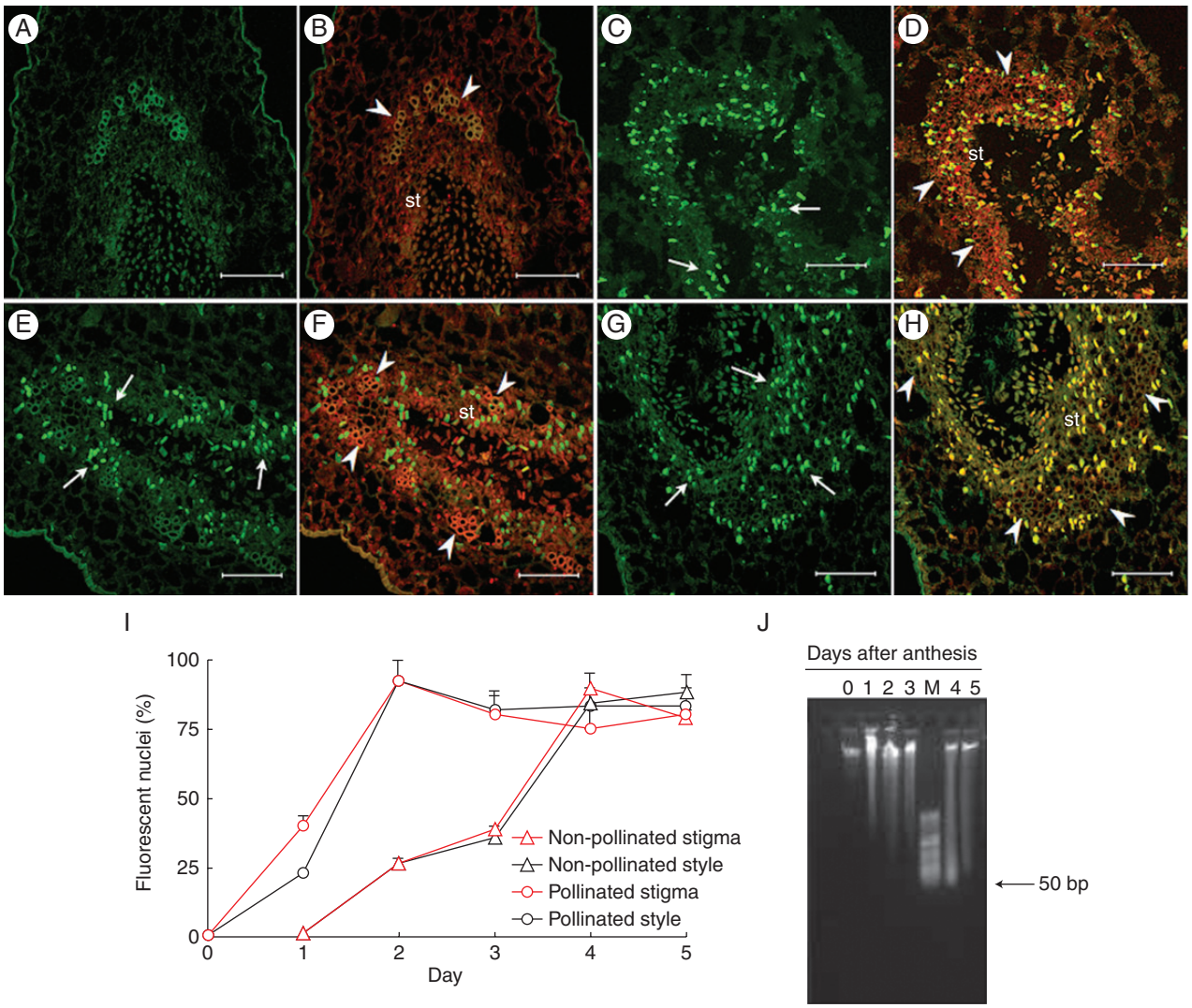

FIG. 4. *In situ* detection of nuclear DNA fragmentation in sections of kiwifruit stigmatic arms by TUNEL assay (A, C, E, G) and counterstained with propidium iodide (B, D, F, H). (A–D) Non-pollinated stigmatic arms sectioned at the level of the stigma showing no nuclei with a positive TUNEL reaction on the first day after anthesis in (A, B), but reaching the maximum number of TUNEL-positive nuclei (arrow) on the fourth day in (C, D). (E–H) Pollinated stigmatic arms sectioned at the level of the stigma showing TUNEL-positive nuclei (arrow) from the first day after anthesis in (E, F), and reaching the maximum number of reactive nuclei on the second day in (G, H). (I) Percentage of TUNEL-reactive nuclei in sections at the levels of the stigma and the base of style from non-pollinated and pollinated flowers. Data represent the percentage (mean ± s.e.) of TUNEL-reactive nuclei from a total of 100 nuclei stained with propidium iodide and counted in at least two stigmatic arms per day and per treatment. (J) Agarose (0·8 %) gel electrophoresis of total DNA isolated from the stigmatic arms of pollinated kiwifruit flowers collected from 0 to 5 d after anthesis. Scale bars (A–H) = 75 μm. Abbreviations: st, secretory tissue; M, HyperLadder II DNA molecular marker of low molecular weight (50–2000 bp). Arrowheads indicate vascular tissue in (B, D, F, H).

No cells of the secretory tissue showing a positive TUNEL reaction were detected in non-pollinated stigmas either at anthesis or 1 d after anthesis (Fig. 4A, B). A significant percentage of nuclei with a positive reaction (25 %) could be observed in non-pollinated stigmas from 2 d after anthesis onwards (Fig. 4I), increasing significantly to a maximum 4 d after anthesis (Fig. 4C, D), when up to 88 % of visible nuclei were TUNEL positive (Fig. 4I).

In the cells of the secretory tissue of stigmas from pollinated flowers, a significantly higher percentage of TUNEL-positive nuclei (40 %) with respect to anthesis was already observed from the first day after anthesis (Fig. 4E, F, I). In fact, the highest percentage of TUNEL-positive nuclei (92 %) was observed on the second day after anthesis (Fig. 4G–I). These results show (Fig. 4I) that the maximum number of TUNEL-positive nuclei was detected 2 d earlier in pollinated stigmas (second day after anthesis) than in non-pollinated stigmas (fourth day after anthesis).

In the cells of the transmitting tissue of styles from non-pollinated flowers (Fig. 4I), TUNEL-positive nuclei were detected with the same chronological sequence as in the secretory tissue of non-pollinated stigmas. However, an important difference was observed in pollinated flowers. On the first day after anthesis, 40 % TUNEL-reactive nuclei could already be observed in the cells of the stigma secretory tissue, while on this day only 25 % TUNEL-reactive nuclei were detected in cells of the transmitting tissue in the base of the style (Fig. 4I). From the second day after anthesis onwards, the number of TUNEL-positive nuclei was the same in both pollinated stigmas and styles (Fig. 4I).

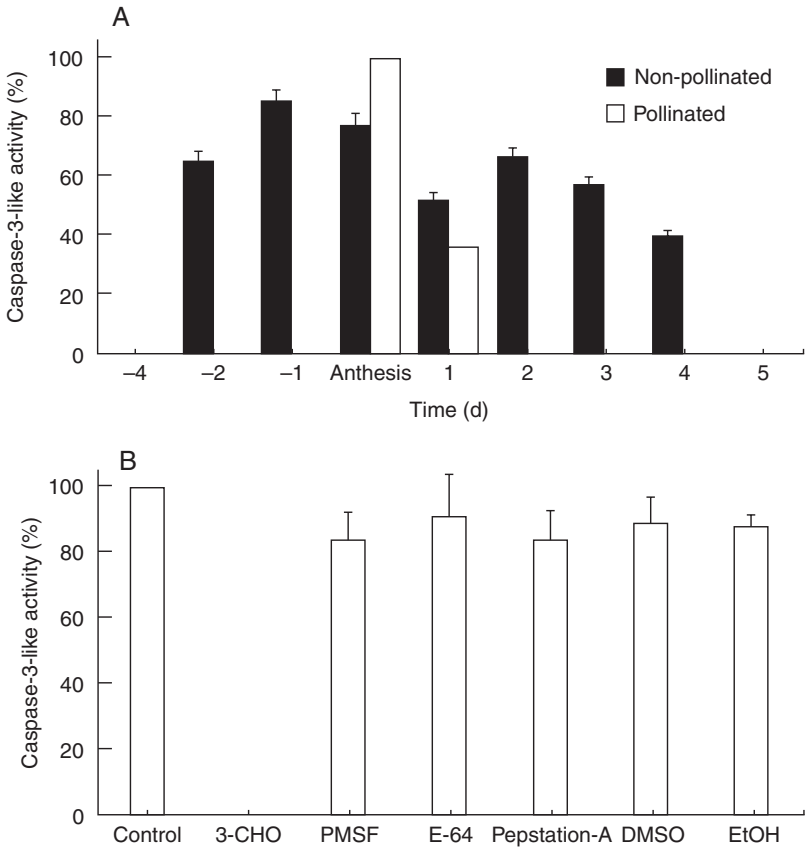

FIG. 5. Caspase-3-like activity in protein extracts from the stigmatic arms of non-pollinated and pollinated kiwifruit flowers collected from 4 d before until 5 d after anthesis. (A) Caspase-3-like activity; (B) caspase-3-like activity in protein extracts from stigmatic arms at anthesis incubated without inhibitor (control) or in the presence of different inhibitors. Data represent the percentage with respect to the maximum activity (mean ± s.e.) of three independent experiments, each performed using three protein extractions per day and per treatment, with spectrophotometric measurements made in duplicate. Abbreviations: 3-CHO, Ac-DEVD-CHO (caspase-3 inhibitor); DMSO, dimethylsulfoxide; E-64, *trans*-epoxysuccinyl-L-leucylamido (4-guanidino) butane; EtOH, ethanol; Pep-A, pepstatin; PMSF, phenylmethylsulfonyl fluoride.

In addition, genomic DNA was extracted from the stigmatic arms of pollinated and non-pollinated flowers and separated by electrophoresis using several different gel matrices. The best resolution was obtained using 0·8 % agarose which allowed observation of a smear from the second day after anthesis when using DNA from non-pollinated flowers, which was more evident by the fourth day (data not shown). In pollinated flowers, a smear was observed from the first day after anthesis, with an accumulation of small fragments between 50 and 300 bp by the fourth day, although an evident laddering was not observed (Fig. 4J).

Caspase-3-like activity assay

Caspase-3-like activity (DEVDase activity), assayed with the caspase-3 substrate Ac-DEVD-pNA, was not detected in leaves or in closed flower buds. Stigmatic arms from flowers collected 4 d before anthesis did not show any activity. DEVDase activity was detected in stigmatic arms of flowers collected from 2 d before anthesis (Fig. 5A). From anthesis, non-pollinated and pollinated stigmatic arms presented a significant decrease in DEVDase activity with respect to that detected at anthesis (Fig. 5A). In particular, DEVDase activity was not detected in pollinated flowers from 2 d after anthesis onwards.

To identify the specific proteolytic enzymatic activity, protein extracts were pre-incubated with Ac-DEVD-CHO (a specific, reversible caspase-3 inhibitor), different types of protease inhibitors and solvents. DEVDase protease activity was inhibited by Ac-DEVD-CHO, while the general protease inhibitors or solvents had no significant effect on this activity (Fig. 5B).

DISCUSSION

In this study, we examined whether PCD plays a role in the EPP and progamic phase in kiwifruit female flowers. We assayed the morphological, biochemical and molecular hallmarks of PCD in the stigmatic arms from non-pollinated and pollinated female flowers just before anthesis and during the subsequent days until the end of the EPP.

From anthesis, the stigmatic arms became gradually brown from the stigma to the base of the style; this browning was accompanied by changes at the histological level (Fig. 1). At anthesis, the stigma sections of non-pollinated flowers showed a secretory tissue with cells rich in starch reserves and a conspicuous extracellular secretion that allows stigmas to prepare to receive pollen grains. During the following days, a progressive cell degradation was observed, fitting with the EPP in this species, and this has

been considered as a mechanism against pathogen infection (González *et al*., 1995*a*, *b*).

In pollinated flowers, these changes began at the stigma on the first day after anthesis, and at the style on the second day after anthesis, fitting with pollen tube passage through the stigma and style, and being accompanied by the disappearance of the extracellular secretion. The presence of an abundant secretion all along the pistilar tract and its subsequent disappearance after passage of the pollen tube have been discussed previously in terms of its possible implication in the high reproductive success of this species (González *et al*., 1996; Howpage *et al*., 1998).

The analysis using TEM of the ultrastructure of the secretory tissues (Fig. 2) allowed a progressive depletion of starch, increase in vacuolization, shrinkage of the protoplast without cell wall degradation, mitochondrial swelling and the rupture of the tonoplast to be detected in their cells. All of these changes were consistent with the end of the EPP in non-pollinated stigmas (4 d after anthesis) and pollen tube passage in pollinated stigmas (2 d after anthesis). Swollen ER was also observed in both non-pollinated and pollinated stigmas. Although this is not generally regarded as a hallmark feature of PCD, Geitmann *et al*. (2004) suggested that a swollen ER may be a useful indicator in certain plant cell types undergoing PCD, such as degenerating tapetal cells, microspore mother cells or differentiating xylem vessels. In contrast, the Golgi apparatus showed a nearly intact structure even in the advanced stages of cell death, as was previously described by Domínguez *et al*. (2001) during nucellus deterioration in wheat.

Another feature of PCD described in plants is chromatin condensation (van Doorn and Woltering, 2005), which can be observed by staining with DAPI. Here DAPI staining of nuclei of stigma secretory tissue revealed a gradual condensation of the chromatin, with nuclei becoming progressively tubular in shape (Fig. 3), as previously described by Cao *et al*. (2003). In addition, a remarkable reduction in the number of nuclei (50 %), as reported in other systems undergoing PCD (Cao *et al*., 2003; Casani *et al*., 2009), was observed 4 d after anthesis in the secretory tissue of non-pollinated stigmas, consistent with the end of the EPP. However, in pollinated flowers, a reduction in the number of nuclei was already initiated in the stigma (20 %) from the first day after anthesis, reaching 45 % on the second day, when the remaining nuclei were bright due to chromatin condensation. Reduction of nuclei in pollinated stigmatic arms occurs 2 d before that in those which were not pollinated, in agreement with the proposed role of pollination as an inducer of cell death, a means of providing a biochemically richer and physically more accommodating medium for pollen tube penetration (Cheung, 1996). In addition, nucleus reduction occurs from the first day in the stigma but only from the second day in the style, consistent with the passage of the pollen tube at the respective structures.

Additional evidence of PCD, as suggested by TEM analysis and DAPI staining, was provided by the evaluation of DNA cleavage using the TUNEL assay (Fig. 4). When non-pollinated stigmatic arm sections were subjected to the TUNEL assay, it was possible to observe an ongoing process of DNA fragmentation in the nuclei. The increase in TUNEL-positive nuclei was evident from the second day after anthesis (25 % of nuclei were TUNEL reactive), reaching the highest level 4 d after anthesis at both the stigma and the base of the style. However, non-pollinated and pollinated flowers were remarkably out of phase because a high percentage of TUNEL-positive nuclei was observed in pollinated stigmas from the first day after anthesis, with approx. 40 % of nuclei being TUNEL positive and the highest level being reached only 2 d after anthesis (92 %). Furthermore, a remarkable difference was observed in pollinated stigmatic arms between the stigma and the style because, in the style, only 25 % of nuclei were TUNEL positive on the first day after anthesis. On the second day, almost all nuclei were reactive to the TUNEL assay in both pollinated stigmas and styles. The gradual increase of TUNEL-positive nuclei observed in the different stages supports the hypothesis that DNA degradation is a temporally regulated process, as proposed by Love *et al*. (2008), which accompanies the progressive death of the secretory cells of the stigmatic arm during the EPP or pollen tube growth.

On the other hand, the acceleration of DNA cleavage in pollinated vs. non-pollinated stigmatic arms and its occurrence according to pollen tube growth agree with the findings of other authors (Wu and Cheung, 2000; Hiratsuka *et al*., 2002; Serrano *et al*., 2010), leading to the conclusion that female tissues interacting with pollen or pollen tubes undergo a dramatic deterioration, including cell death. Wang *et al*. (1996) reported that the transmitting tissue in non-pollinated styles of tobacco does not reach the same level of deterioration – even after ethylene treatment – as that in pollinated styles, suggesting that pollen tube penetration is necessary to elicit the cell deterioration processes to its full extent.

Another hallmark considered as an indicator of PCD was oligonucleosomal fragmentation of chromosomal DNA (Wredle *et al*., 2001). However, Coimbra *et al*. (2004) reported that chromatin can break in a way that yields 3′-OH groups (detected by TUNEL) but not in a way that gives nucleosomal bands of about 180 bp; hence, not all TUNEL-positive cells will show laddering in an electrophoresis gel. Collazo *et al*. (2006) showed that the size of the DNA fragments can vary from 140 bp to as large as 50 000 bp. Also, Reape and McCabe (2008) reported DNA cleavage into either large or small fragments as evidence of PCD. The results of these previous reports agree with the extensive DNA cleavage observed as a smear pattern in kiwifruit stigmatic arms (Fig. 4H) starting from the first and the second day after anthesis in pollinated and non-pollinated flowers, respectively. Evidence of DNA degradation was also recently reported in PCD programmes detected in the stigmas of *Olea europaea* under free pollination (Serrano *et al*., 2010) and in the development of maternal seed tissue in barley (Radchuk *et al*., 2011).

The involvement of caspases, a family of cysteine-dependent aspartate-specific proteases known to have important functions in animal PCD, is controversial in plant PCD because there are no evident homologues of caspases in plants (Vartapetian *et al*., 2011). However, caspase inhibitors can block PCD in plants, and most instances of plant PCD are associated with the induction of caspase-like activities (reviewed in Sanmartín *et al*., 2005). Caspase-3-like enzymes have been reported to be involved in reproductive processes in plants, such as pollen–pistil interaction in *Olea* (Serrano *et al*., 2010), self-incompatibility in *Papaver* (Bosch and Franklin-Tong, 2007, 2008), suspensor degeneration during embryogenesis in *Leguminosae* (Wredle *et al*., 2001; Lombardi *et al*., 2007; Endo, 2012), cotyledon dismantling during seed germination in *Vigna* (Egorova *et al*., 2010) and megagametophyte degeneration post-germination in *Araucaria* (Casani

et al., 2009). In our system (Fig. 5), caspase-3-like activity was higher until anthesis and then decreased significantly. Various caspase inhibitors were assayed to establish the specificity of this activity. The enzyme activity was significantly inhibited by Ac-DEVD-CHO (a specific inhibitor of caspase-3), while other protease inhibitors had little or no effect on this DEVDase activity, in agreement with other reports (Danon *et al*., 2004; Qu *et al*., 2009; Egorova *et al*., 2010). These data further reinforce the results obtained with other hallmarks of the involvement of PCD in the stigmatic arms during the EPP and the pollen–pistil interaction in kiwifruit. In addition, we showed here that caspase-3-like activity precedes DNA degradation in kiwifruit pistils, as reported in other plant systems (Danon *et al*., 2004; Lam, 2004; Serrano *et al*., 2010).

Our data show characteristics established as markers for PCD in non-pollinated and pollinated stigmatic arms of kiwifruit. Data obtained using the TUNEL assay and electrophoretic analysis suggest that the nuclear DNA of the secretory cells had undergone cleavage, which is one of the prominent hallmarks of PCD. The DAPI staining showed chromatin condensation and nuclear loss. Moreover, ultrastructural studies showed a gradual decrease in the volume of the cytoplasm with a concomitant increase in the volume occupied by vacuoles, and, in a final step, swelling of the mitochondria, collapse of the vacuolar membrane and protoplast shrinkage. Finally, caspase-3-like activity was also detected.

Based on the findings described above, we propose that a PCD programme may be involved in the events described in the stigma and the style of kiwifruit flowers from the day of anthesis until the end of the EPP. This PCD programme produced a progressive deterioration of the secretory tissues, providing a physically and biochemically appropriate medium supporting the growth of >1200 pollen tubes (González *et al*., 1996; Howpage *et al*., 1998); however, the deterioration of the tissues would also impair the germination of new pollen arriving at the stigma, thus shortening the EPP to only 4 d after anthesis in this species (González *et al*., 1995*a*, *b*).

The results obtained in kiwifruit stigmatic arms upon pollination support the idea that PCD might be accelerated by pollination, which disrupts the timing with respect to non-pollinated flowers. Hallmarks of PCD were observed in the stigmas of pollinated flowers on the second day after anthesis, and 2 d later (4 d after anthesis) in non-pollinated stigmas. In addition, in pollinated flowers, PCD signs were present sooner at the stigmas than at the base of the style, consistent with pollen tube growth. These observations point to the involvement of PCD during the progamic phase, as was previously described by other authors (Domínguez *et al*., 2001; Hiratsuka *et al*., 2002; Serrano *et al*., 2010).

Understanding the mechanisms of control with pivotal roles in the regulation of PCD in kiwifruit stigmatic arms could have a great impact in improving harvest, since the extension of the EPP would allow the percentage of fruits with a high number of seeds and hence with more commercial value to be increased.

ACKNOWLEDGEMENTS

This research was supported by the Xunta de Galicia (Regional Government of Galicia, Spain; project PGIDIT 04RAG291002PR). We thank Kiwi Atlántico S.A. for providing the plant material. We thank Dr P. Testillano (Centro de Investigaciones Biológicas, CSIC, Madrid, Spain) for her generous advice with TUNEL protocols, and Dr M. Herrero (Aula Dei Experimental Station, CSIC, Zaragoza, Spain) for her help in the interpretation of TEM analyses. We also thank M. S. Costa for her expert photographic assistance, and B. Lueiro for her technical assistance. This is a contribution of the Interuniversity Research Group in Biotechnology and Reproductive Biology of Woody Plants (BioVitAc Research group, code 09IDI1705).

LITERATURE CITED

Bosch M, Franklin-Tong V. 2007. Temporal and spatial activation of caspase-like enzymes induced by self-incompatibility in *Papaver* pollen. *Proceedings of the National Academy of Sciences, USA* **104**: 18327–18332.

Bosch M, Franklin-Tong V. 2008. Self-incompatibility in *Papaver*: signalling to trigger PCD in incompatible pollen. *Journal of Experimental Botany* **59**: 481–490.

Bosch M, Poulter NS, Perry RM, Wilkins KA, Franklin-Tong V. 2010. Characterization of a legumain/vacuolar processing enzyme and YVADase activity in *Papaver* pollen. *Plant Molecular Biology* **74**: 381–393.

Cao J, Jiang F, Sodmergen, Cui K. 2003. Time-course of programmed cell death during leaf senescence in *Eucommia ulmoides*. *Journal of Plant Research* **116**: 7–12.

Casani S, Fontanini D, Capocchi A, Lombardi L, Galleschi L. 2009. Investigation on cell death in the megagametophyte of *Araucaria bidwillii* Hook. post-germinated seeds. *Plant Physiology and Biochemistry* **47**: 599–607.

Cheung AY. 1996. The pollen tube growth pathway: its molecular and biochemical contributions and responses to pollination. *Sexual Plant Reproduction* **9**: 330–336.

Coimbra S, Torrao L, Abreu I. 2004. Programmed cell death induces male sterility in *Actinidia deliciosa* female flowers. *Plant Physiology and Biochemistry* **42**: 537–541.

Collazo C, Chacón O, Borras O. 2006. Programmed cell death in plants resembles apoptosis of animals. *Biotecnología Aplicada* **23**: 1–10.

Danon A, Rotari VI, Gordon A, Mailhac N, Gallois P. 2004. Ultraviolet-C overexposure induces programmed cell death in *Arabidopsis*, which is mediated by caspase-like activities and which can be suppressed by caspase inhibitors, p35 and defender against apoptotic death. *Journal of Biological Chemistry* **279**: 779–787.

Della Mea M, Serafini-Fracassini D, Del Duca S. 2007. Programmed cell death: similarities ad differences in animals and plants. A flower paradigm. *Amino Acids* **33**: 395–404.

Domínguez F, Moreno J, Cejudo FJ. 2001. The nucellus degenerates by a process of programmed cell death during the early stages of wheat grain development. *Planta* **213**: 352–360.

van Doorn WG, Woltering EJ. 2005. Many ways to exit? Cell death categories in plants. *Trends in Plant Science* **10**: 117–122.

van Doorn WG, Beers EP, Dangl JL, *et al*. 2011. Morphological classification of plant cell deaths. *Cell Death and Differentiation* **18**: 1241–1246.

Egorova VP, Zhao Q, Lo Y-S, *et al*. 2010. Programmed cell death of the mung bean cotyledon during seed germination. *Botanical Studies* **51**: 439–449.

Ellis RE, Yuan J, Horvitz HR. 1991. Mechanisms and functions of cell death. *Annual Review of Cell Biology* **7**: 663–698.

Endo Y. 2012. Characterization and systematic implications of the diversity in timing of programmed cell death of the suspensors in Leguminosae. *American Journal of Botany* **99**: 1399–1407.

Falasca G, D'Angeli S, Biasi R, *et al*. 2013. Tapetum and middle layer control male fertility in *Actinidia deliciosa*. *Annals of Botany* **112**: 1045–1055.

Geitmann A, Franklin-Tong VE, Emons AC. 2004. The self-incompatibility response in *Papaver rhoeas* pollen causes early and striking alterations to organelles. *Cell Death and Differentiation* **11**: 812–822.

González MV, Coque M, Herrero M. 1995*a*. Stigmatic receptivity limits the effective pollination period in kiwifruit. *Journal of the American Society for Horticultural Science* **102**: 199–202.

González MV, Coque M, Herrero M. 1995*b*. Papillar integrity as an indicador of stigmatic receptivity in kiwifruit (*Actinidia deliciosa*). *Journal of Experimental Botany* **46**: 263–269.

González MV, Coque M, Herrero M. 1996. Pollen–pistil interaction in kiwifruit (*Actinidia deliciosa*; *Actinidiaceae*). *American Journal of Botany* **83**: 148–154.

Greenberg JT. 1996. Programmed cell death: a way of life for plants. *Proceedings of the National Academy of Sciences*, *USA* **93**: 12094–12097.

Hara-Nishimura I, Hatsugai N. 2011. The role of vacuole in plant cell death. *Cell Death and Differentiation* **18**: 1298–1304.

Hiratsuka R, Yamada Y, Terasaka O. 2002. Programmed cell death of *Pinus nucellus* in response to pollen tube penetration. *Journal of Plant Research* **115**: 141–148.

Hiscock SJ, Allen AM. 2008. Diverse cell signalling pathways regulate pollen–stigma interactions: the search for consensus. *New Phytologist* **179**: 286–317.

Howpage D, Vithanage V, Spooner-Hart R. 1998. Pollen tube distribution in the kiwifruit (*Actinidia deliciosa* A. Chev. C.F. Liang) pistil in relation to its reproductive process. *Annals of Botany* **81**: 697–703.

Lam E. 2004. Controlled cell death, plant survival and development. *Nature Reviews Molecular Cell Biology* **5**: 305–315.

Lombardi L, Cecarelli N, Picciarelli P, Lorenzi R. 2007. DNA degradation during programmed cell death in *Phaseolus coccineus* suspensor. *Plant Physiology and Biochemistry* **45**: 221–227.

Love AJ, Milner JJ, Sadanandom A. 2008. Timing is everything: regulatory overlap in plant cell death. *Trends in Plant Science* **13**: 589–595.

Pennell RI, Lamb C. 1997. Programmed cell death in plants. *The Plant Cell* **9**: 1157–1168.

Qu G-Q, Liu X, Zhang Y-J, *et al*. 2009. Evidence for programmed cell death and activation of specific caspase-like enzymes in the tomato fruit heat stress response. *Planta* **229**: 1269–1279.

Radchuk V, Weier D, Radchuck R, Weschke W, Weber H. 2011. Development of maternal seed tissue in barley is mediated by regulated cell expansion and cell disintegration and coordinated with endosperm growth. *Journal of Experimental Botany* **62**: 1217–1227.

Reape TJ, McCabe PF. 2008. Apoptotic-like programmed cell death in plants. *New Phytologist* **180**: 13–26.

Reape TJ, Molony EM, McCabe PF. 2008. Programmed cell death in plants: distinguishing between different modes. *Journal of Experimental Botany* **59**: 435–444.

Rogers HJ. 2006. Programmed cell death in floral organs: how and why do flowers die? *Annals of Botany* **97**: 309–315.

Sabatini DD, Bensch K, Barrett RJ. 1963. Cytochemistry and electron microscopy: the presentation of cellular ultrastructure and enzymatic activity by aldehyde fixation. *Journal of Cell Biology* **17**: 19–58.

Sanmartín M, Jaroszewski L, Raikhel NV, Rojo E. 2005. Caspases. Regulating death since the origin of life. *Plant Physiology* **137**: 841–847.

Serrano I, Pelliccione S, Olmedilla A. 2010. Programmed-cell-death hallmarks in incompatible pollen and papillar stigma cells of *Olea europaea* L. under free pollination. *Plant Cell Reports* **29**: 561–572.

Thomas SG, Franklin-Tong V. 2004. Self-incompatibility triggers programmed cell death in *Papaver* pollen. *Nature* **429**: 305–309.

Vartapetian AB, Tuzhikov AI, Chichkova NV, Taliansky M, Wolpert TJ. 2011. A plant alternative to animal caspases: subtilisin-like proteases. *Cell Death and Differentiation* **18**: 1289–1297.

Wang H, Wu HM, Cheung AY. 1996. Pollination induces mRNA poly(A) tail-shortening and cell deterioration in flower transmitting tissue. *The Plant Journal* **9**: 715–727.

Williams JH Jr, Friedman WE, Arnold ML. 1999. Developmental selection within the angiosperm style: using gamete DNA to visualize interspecific pollen competition. *Proceedings of the National Academy of Sciences*, *USA* **96**: 9201–9206.

Wredle U, Walles B, Hakman I. 2001. DNA fragmentation and nuclear degradation during programmed cell death in the suspensor and endosperm of *Vicia faba*. *International Journal of Plant Sciences* **162**: 1053–1063.

Wu H, Cheung AY. 2000. Programmed cell death in plant reproduction. *Plant Molecular Biology* **4**: 267–281.